Proceedings of the 2nd Croatian Conference on Earthquake Engineering - 2CroCEE
Zagreb, Croatia - March 22 to 24, 2023

DOI: https://doi.org/10.5592/CO/2CroCEE.2023.23

EARTHQUAKE PERFORMANCE OF A CULTURAL HERITAGE BUILDING: THE JESUIT COLLEGE IN DUBROVNIK, CROATIA

Aanis Uzair (1), Lars Abrahamczyk (2), Dagoberto Gómez (3), Kinda Elias (4), Ante Vrban (5), Davorin Penava (6), Snježana Markušić (7)

(1) *Research Assistant, Chair of Advanced Structures, Faculty of Civil Engineering, Bauhaus-University Weimar, aanis.uzair@uni-weimar.de*
(2) *Professor, Chair of Advanced Structures, Faculty of Civil Engineering, Bauhaus-University Weimar, lars.abrahamczyk@uni-weimar.de*
(3) *Graduate Student, Chair of Advanced Structures, Faculty of Civil Engineering, Bauhaus-University Weimar, dagogomez08@gmail.com*
(4) *Graduate Student, Chair of Advanced Structures, Faculty of Civil Engineering, Bauhaus-University Weimar, kinda.elias@outlook.com*
(5) *PhD Student, Faculty of Civil Engineering and Architecture Osijek, Josip Juraj Strossmayer University of Osijek, ante.vrban@gfos.hr*
(6) *Professor, Faculty of Civil Engineering and Architecture Osijek, Josip Juraj Strossmayer University of Osijek, ante.vrban@gfos.hr*
(7) *Professor, Department of Geophysics, Faculty of Science, University of Zagreb, markusic@gfz.hr*

Abstract

Cultural heritage buildings generally refer to the ancient structures having high cultural and historical significance. These buildings are constructed using obsolete practices and require special considerations with respect to the lateral resistance, especially in moderate and high seismic regions. This study focuses on the earthquake performance assessment of the Episcopal Seminary Building and Classical Gymnasium (Jesuit College) located in the Old City of Dubrovnik, Croatia (UNESCO World Heritage Site). The construction dates back to 1662 and was developed in different stages until 1765. During this period, Jesuit College suffered damages from two major earthquakes i.e., M7.6 Dubrovnik in 1667 and M6.9 Montenegro in 1979. The material composition, structural drawings, and fundamental frequencies of the building were previously obtained in the framework of the research project "Seismic Risk Assessment of Cultural Heritage in Croatia – SeisRICHerCRO". The material is predominantly composed of irregular stone blocks laid in lime mortar. The structural details such as floor vaults, arches, flexible diaphragms, and spatially irregular openings are numerically modelled using the finite element method. The analytical model is calibrated by performing eigenvalue analysis to compute the material parameters i.e., elastic modulus and density (supported by extensive literature review) that allows the modal frequencies to match with the values obtained from the ambient vibration testing. The seismic performance is then evaluated using the linear analysis procedure in accordance with the current guidelines of the Eurocode 8 and the corresponding Croatian National Annex. For the design earthquake, critical damage zones are identified and recommendations for retrofitting measures are proposed.

Keywords: unreinforced masonry, cultural heritage, finite element model updating, earthquake performance assessment

1. Introduction

Cultural heritage buildings symbolize our history by providing insight into the evolution of our culture and society over a long period of time. These buildings are predominantly built with traditional materials such as masonry and timber and are often exposed to the lack of maintenance, water induced deterioration, foundation settlement, fluctuating environmental loads, floods, and earthquakes [1]. The seismic performance of built cultural heritage is particularly difficult to access and requires detailed knowledge of the material composition, geometrical characteristics, nonlinear effects, connections between different structural elements, stiffness of the horizontal diaphragms, and the building condition [2,3].

Proceedings of the 2nd Croatian Conference on Earthquake Engineering - 2CroCEE
Zagreb, Croatia - March 22 to 24, 2023

DOI: https://doi.org/10.5592/CO/2CroCEE.2023.23

In the case of historical structures, the availability of input data is often limited either by the incompleteness of the archived documents or because of the impracticality to conduct in-situ experiments while preserving the architectural features. In this context, vibration-based techniques to evaluate the structural dynamic response appears particularly attractive [4–6]. In recent years, many studies demonstrate the successful application of Ambient Vibration Tests (AVT) in combination with Finite Element (FE) model updating, for the performance assessment of cultural heritage buildings [7–10]. The model updating process calibrates the unknown structural parameters to minimize the error between experimental and analytical dynamic response i.e., modal frequencies and mode shapes. This process is often accomplished manually through trial and error and becomes cumbersome for complex buildings, causing uncertainty in the estimation of the unknown structural parameters [11].

This paper presents the earthquake performance assessment of the Episcopal Seminary Building and Classical Gymnasium (Jesuit College) using AVT in combination with FE model updating. The Jesuit College was built from 1662 to 1725 and lies in the UNESCO's World Heritage List Old City of Dubrovnik, Croatia. The building is primarily used as an educational institute. The historical seismicity of Dubrovnik shows a considerable seismic potential with the 1667 earthquake considered to be the strongest documented earthquake in the coastal region of Croatia [12]. By its seismic and tectonic potential, it is also the most striking area in Croatia with estimated maximum possible magnitude of 7.5. Historic data note about ten earthquakes in the region with intensity of VIII or more ºMCS out of which the most significant one is the 1667 earthquake of X °MCS [13].

2. Material and Methods

2.1 Episcopal Seminary Building and Classical Gymnasium

The Episcopal Seminary Building and Classical Gymnasium is one of the city's oldest educational institutes (shown in Fig. 1). The construction dates back to 1662 and was further developed over the years until 1725. The internal walls are predominantly composed of irregular stone masonry laid in lime-mortar. The deterioration of exterior walls exposes the variability in the material composition mainly attributed to the different construction stages and maintenance over the years, as shown in Fig. 2. The geometry, structural details, and damage conditions were assessed previously through a qualitative site inspection in part of the research project SeisRICHerCRO [14]. The roof structure is predominantly made of wood with no precise information available regarding the material properties. Wooden beams supporting the flexible floor system are supported on top of masonry corbels without embedment into the adjacent walls. The most important structural and architectural feature of this building is the different type of vaults supporting the floor slab. Fig. 3 shows the location of the cross and barrel vaults laid in stone masonry. In addition, the top floor also features tensile tie rods, providing additional lateral support to the parallel walls in the out-of-plane direction.

Figure 1. Episcopal Seminary Building and Classical Gymnasium, Dubrovnik, Croatia [15].

Proceedings of the 2nd Croatian Conference on Earthquake Engineering - 2CroCEE
Zagreb, Croatia - March 22 to 24, 2023

DOI: https://doi.org/10.5592/CO/2CroCEE.2023.23

Figure 2. Materials characteristics of the external walls (composite clay bricks and stone masonry of variable sizes).

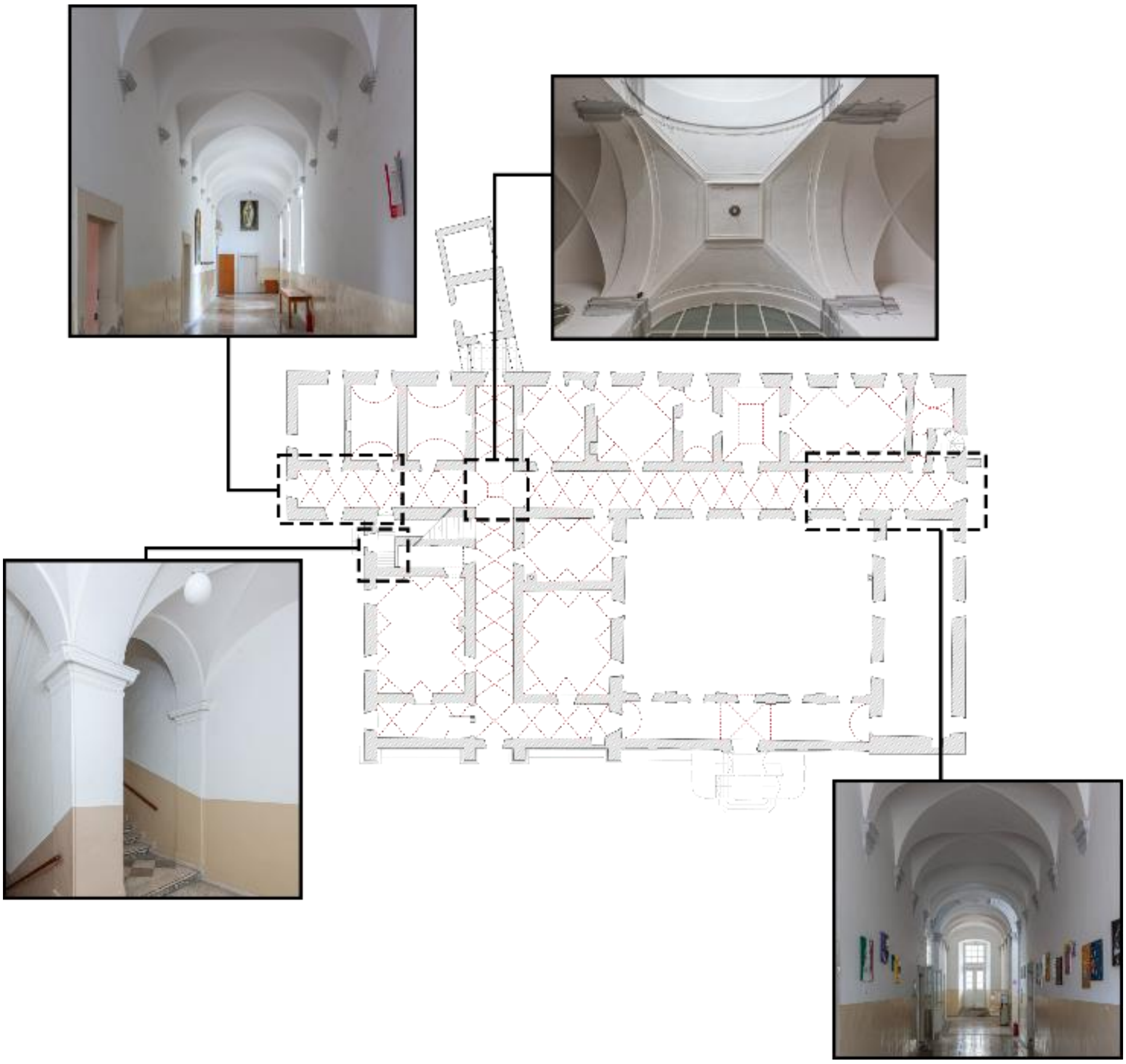

Figure 3. Location and types of different vault systems in the Jesuit College.

Proceedings of the 2nd Croatian Conference on Earthquake Engineering - 2CroCEE
Zagreb, Croatia - March 22 to 24, 2023

DOI: https://doi.org/10.5592/CO/2CroCEE.2023.23

2.2 Ambient Vibration Testing

The fundamental frequencies in North-South (NS) and East-West (EW) directions were previously determined using AVS in part of the research project SeisRICHerCRO [14]. Three sensors located on the first floor recorded continuous data with a sampling rate of 128Hz for three consecutive days. Fourier Amplitude Spectra (FAS) for the two horizontal components and the Horizontal to Vertical Spectral Ratio (HVSR) is used to obtain the fundamental frequencies in the NS and EW direction as shown in Table 1. It is important to note that for this study, only the fundamental frequencies were obtained without the identification of structural mode shapes.

Table 1 – Fundamental frequencies [Hz] in the NS and EW direction obtained from the ambient vibration testing [16].

Frequency	Lower Bound	Average	Upper Bound
$f_{NS,ref}$	6.34	7.88	8.28
$f_{EW,ref}$	4.72	5.38	6.01

3. Finite Element Model Updating

The building is analysed utilizing the macro modelling approach, where the walls and vaults are modelled using solid elements and a linear masonry material property. The interaction among building sections built in different years is neglected and the basement is excluded from the structural model since its contribution to the fundamental period is negligible. Timber floors and the roof structure are modelled as equivalent flat shell elements allowing the transfer of bending effects due to the gravitational loads and in plane stresses, simulating the level of rigidity associated with a flexible diaphragm. The in-plane stiffness of the wooden structure and its components is represented by an equivalent Young's Modulus. The spiral staircase is neglected from the modelling since the surrounding walls are considerable rigid. The iron tie-rods are included in the model as regular truss elements carrying a pre-stressing axial force and allowing deformations only along the element axis. The mesh consists of hexahedral and quadrilateral elements for the solids and flat shells respectively. The basic mesh element size is 0.5m with a 65% transition smoothness for the edges and corners shaped by the vaults as shown in Fig. 4. The final mesh has a total of 119'306 nodes from which 2'659 are the restricted nodes at the base and, 184'821 elements distributed as 173'628 solids, 11'176 shells and 17 trusses.

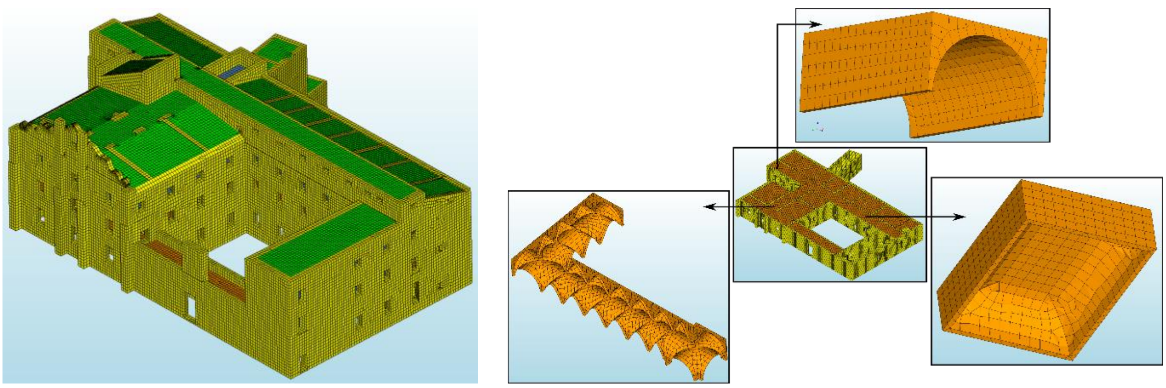

Figure 4. FEM mesh with hexahedral and quadrilateral elements with an approximate size of 0.5m.

The initial material properties used for the FE model updating are collected from the literature in conjunction with the observations made during the qualitative site inspection in part of the research project SeisRICHerCRO [14]. Starting with a reference set of material properties not only provides a physical sense to the calibrated values but also optimizes the time required for convergence in case of

Proceedings of the 2nd Croatian Conference on Earthquake Engineering - 2CroCEE
Zagreb, Croatia - March 22 to 24, 2023

DOI: https://doi.org/10.5592/CO/2CroCEE.2023.23

manual updating. The possible range of values considered for the material properties are summarized in Table 2. Since the model updating is performed manually, the unknown material parameters are restricted to the elastic modulus (E_{ref}), unit weight (p_{ref}) and poison ratio (v_{ref}), reducing uncertainty in the calibrated parameters. Free vibration Eigen Value Analysis is performed for a total of 21 parameter combinations to minimize the error between numerical and experimental dynamic response. The error obtained at the end of each model updating run is shown in Fig. 5.

Table 2 – Range of material properties considered for the FE model updating [17].

Parameter	Lower Bound	Average	Upper Bound
$E_{,ref}$ [MPa]	2000	2650	3300
$p_{,ref}$ [kg/m^3]	2000	2350	2700
$v_{,ref}$	0.10	0.20	0.30

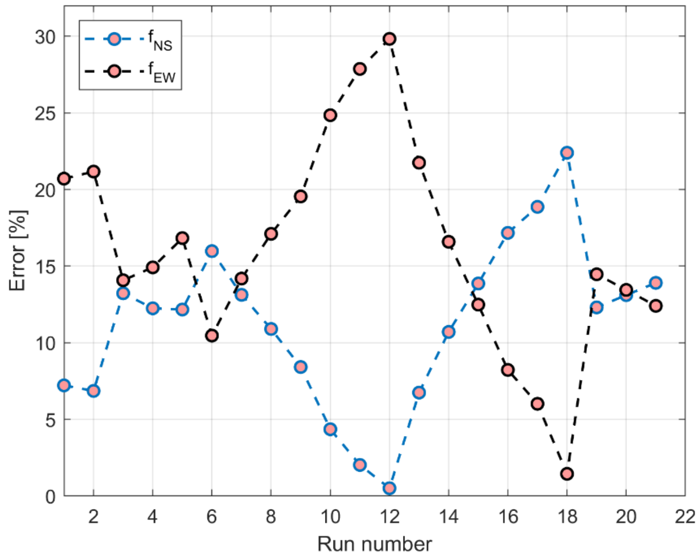

Figure 5. Error obtained in the NS and EW frequencies for each run of the FE model updating process.

The analytical frequencies with the least error are 6.05Hz corresponding to the NS (mode 2) and 6.79Hz corresponding to the EW (mode 5) direction respectively, as shown in Table 3. The most relevant mode shapes are shown in Fig. 6. Mode shape 1 has the lowest frequency representing the local vibration mode of the cantilever clock wall, anticipating tensile stresses concentration at the base of the wall. Mode shape 2 and 5 represents the translational modes in NS and EW directions respectively.

Table 3 – Modal frequencies obtained for the calibrated material properties.

Mode	Period [s]	Frequency [Hz]	Mass Participation [%]		Mode	Period [s]	Frequency [Hz]	Mass Participation [%]	
			EW	NS				EW	NS
1	0.193	5.18	0.0037	3.3227	6	0.145	6.88	11.8290	0.0037
2	0.165	6.05	0.0521	61.2830	7	0.129	7.78	2.5400	4.6558
3	0.155	6.47	0.0016	0.0055	8	0.121	8.24	1.7574	0.0859
4	0.154	6.49	0.0209	0.0043	9	0.119	8.42	0.0083	0.0054
5	0.147	6.79	56.1830	0.0101	10	0.112	8.94	0.0137	0.7164

Proceedings of the 2nd Croatian Conference on Earthquake Engineering - 2CroCEE
Zagreb, Croatia - March 22 to 24, 2023

DOI: https://doi.org/10.5592/CO/2CroCEE.2023.23

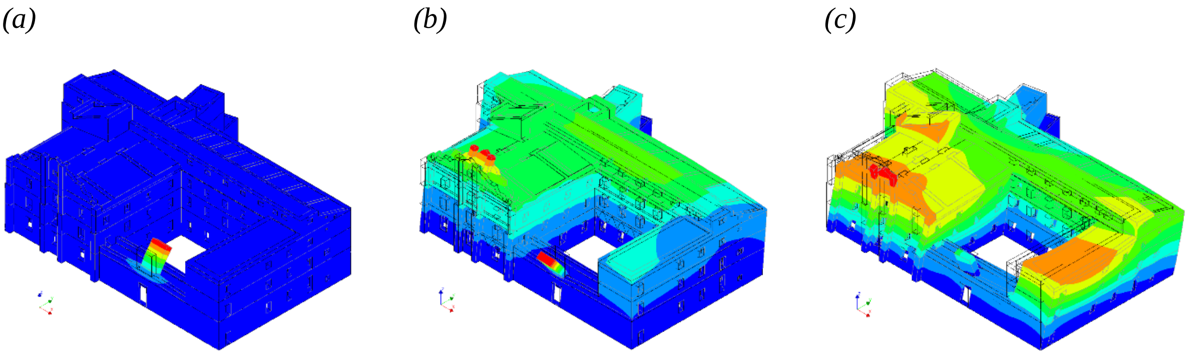

Figure 6. Relevant mode shapes obtained using the calibrated finite element model. a) Mode shape 1 (local mode, f = 5.18 Hz); b) Mode shape 2 (global mode, f = 6.05 Hz); c) Mode shape 5 (global mode, f = 6.79 Hz).

4. Earthquake Performance Assessment

4.1 Seismic Hazard Definition

The seismic hazard is defined according to the Eurocode 8 guidelines for assessment and retrofitting of buildings using the nationally defined reference peak ground acceleration (a_{gR}) for the no-collapse requirement, corresponding to a return period T_{NcR} of 475 years [18,19]. Recent studies describe the site conditions of Dubrovnik as cretaceous dolomitic limestone and quaternary clay, with sand sediments of up to 5m thick, classifying the site as soil type A with an a_{gR} of 0.30g [20,21].

4.2 In-Plane Assessment

The in-plane lateral capacity is evaluated using permanent, imposed, seismic and snow loads. The load combination (LC1) acting mainly in the X-direction, additionally includes the factored Y-direction component as well. The opposite occurs in the case of LC2 acting mainly in the Y-direction. Both the load combinations include the accidental torsional effects according to the Eurocode 8. The tensile ($f_{t,CF}$ = 0.30MPa) and compressive ($f_{t,CF}$ = 0.30MPa) elastic stress limits of the masonry material are reduced using a confidence factor (CF) equal to 1.35 corresponding to the knowledge level KL_1 according to Eurocode 8. The tensile and compressive elastic stress limits are given by Eq. (1) and (2).

$$f_{t,CF} = \frac{f_t}{CF} = \frac{0.39}{1.35} = 0.30\ MPa \tag{1}$$

$$f_{c,CF} = \frac{f_t}{CF} = \frac{6.90}{1.35} = 5.0\ MPa \tag{2}$$

The principal tensile and compressive stresses due to the two load combinations i.e., LC1 and LC2 are shown in Fig. 7. The color scale is bounded such that the red color represents the regions where maximum tensile stress is higher than $f_{t,CF}$ and cracking is expected to occur. High stress is observed around the corners of the opening and at the piers between adjacent openings. Comparable high stresses are obtained in the wall segments having fewer openings, representing concentrated shear stresses. The perpendicular walls show considerable tensile stresses due to Out-of-Plane (OoP) deformations especially in the upper portions of the walls where the cantilever motion is not restricted. The principal compressive stresses from Fig. 7b shows high stresses in the columns of the north facade at the east wing because of the overturning moment caused by the direction of the seismic forces. Moreover, the upper part of the columns resist the compression generated by the OoP bending of the cantilever wall in the north facade, indicated by stresses in the light green color. High compressive stresses are also located at the base of the clock wall, since this wall is identified as critical zone due to the OoP bending; previously identified from the local vibration mode shown in Fig. 6a.

DOI: https://doi.org/10.5592/CO/2CroCEE.2023.23

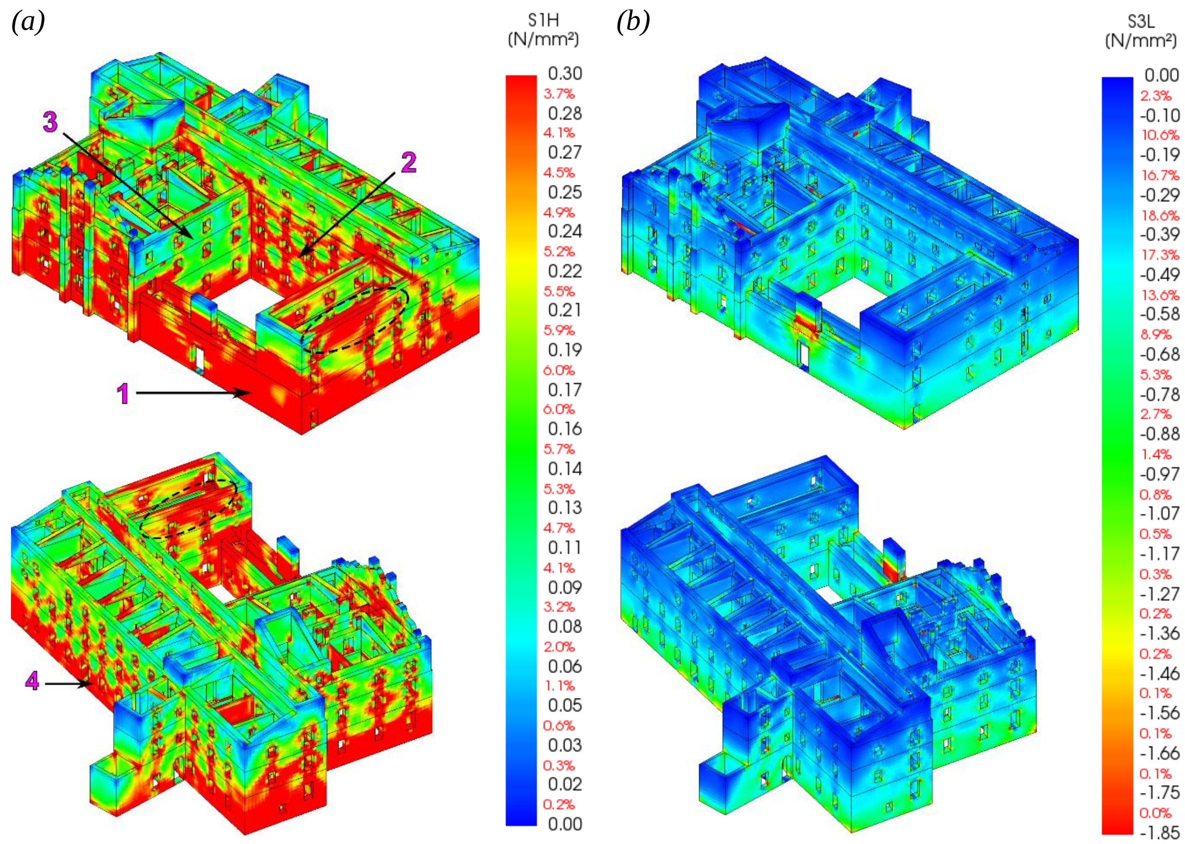

Figure 7. Resulting principal tensile and compressive stresses. a) Principal tensile stress (S1H) resulting from LC1; b) Principal compressive stress (S3L) resulting from LC2.

The shear stress concentration for the two load combinations is shown in Fig. 8. The XZ plane show high shear stresses (SZXH) between the openings of the north facade with visible diagonal concentration at the corners of the north wing walls. The north and south facades of the south wing also indicate shear stresses with diagonal trajectory located at the piers between the openings. Similar results are obtained for the stresses in the YZ plane (SYZH), with the particularity that the stresses are higher on the walls at the east wing because of the high mass resulting in higher seismic forces. Additionally, high shear stresses are obtained at the base of the clock wall in the YZ plane due to the OoP deformation.

Fig. 9 shows the tensile stresses in the masonry vaults in both X and Y directions. For the stresses in the X direction (SXX), the higher tensile stresses are developed near the wall connection and along the longitudinal direction of the vault in the east wing hallway. It is analogous in Fig. 9b for the stresses in Y direction (SYY) where, the development of stresses goes along the cross vault of the hallway in the south wing. The response is repeated at the entrance in the north wing, and additionally in some regions along the vault, preventing the lateral walls to bend separately out of the plane. The stresses are generated when the vault is oriented perpendicular to the direction of the seismic forces. Tensile stresses SXX also develop in the vault of the north wing, at the regions near the connections with the east and west wings. The latter is due to the pulling force generated by the east and west wings when the earthquake occurs in the X direction.

The numerical model is further evaluated for increasing values of a_{gR} corresponding to different seismic zones in Croatia. Fig. 10 shows a gradual increase of tensile stresses (S1H) where, the limit $f_{t,cF}$ of 0.30MPa is exceeded. For low seismic hazard level (a_{gR} = 0.10g) the stresses are below the limit in practically all areas. The limit is exceeded for a_{gR} = 0.20g in localized regions such as openings and critical corners.

DOI: https://doi.org/10.5592/CO/2CroCEE.2023.23

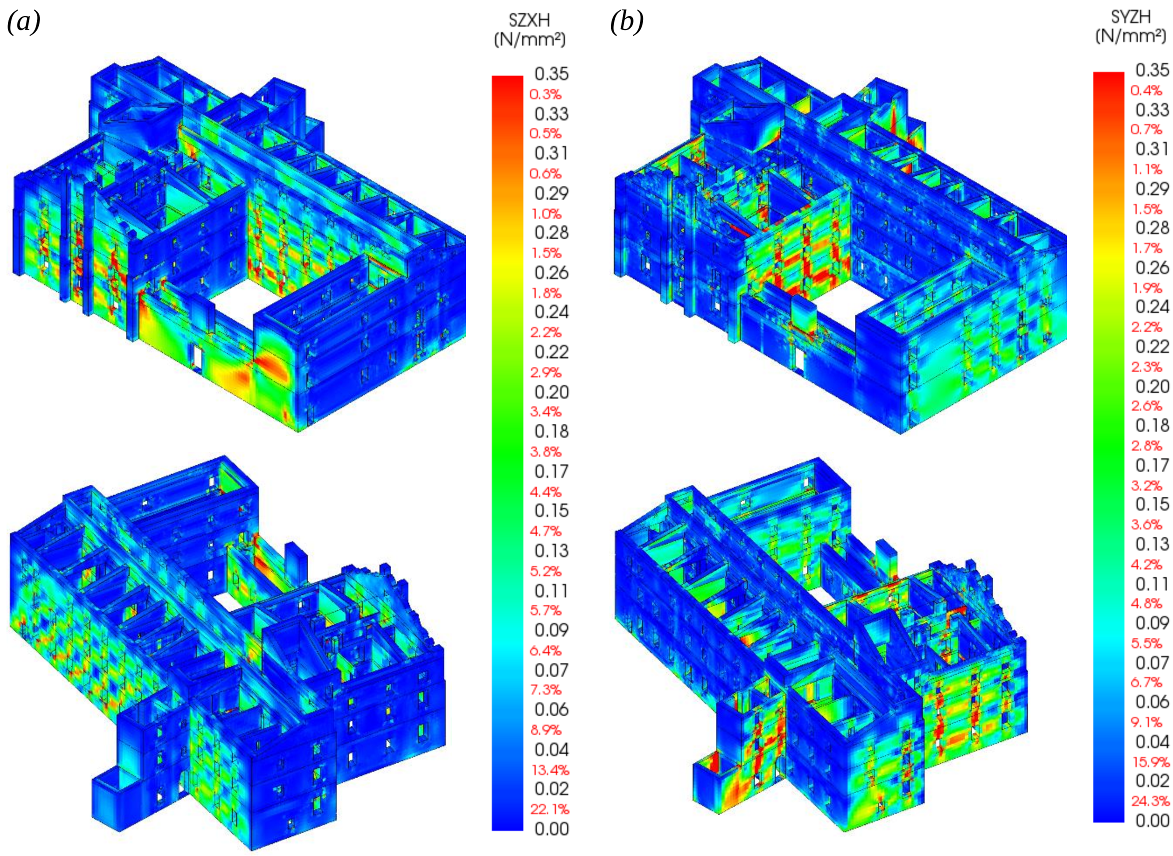

Figure 8. Resulting shear stresses in the global XZ and YZ directions. a) Shear stress in XZ plane (SZXH) resulting from LC1; b) Shear stress in YZ plane (SYZH) resulting from LC2.

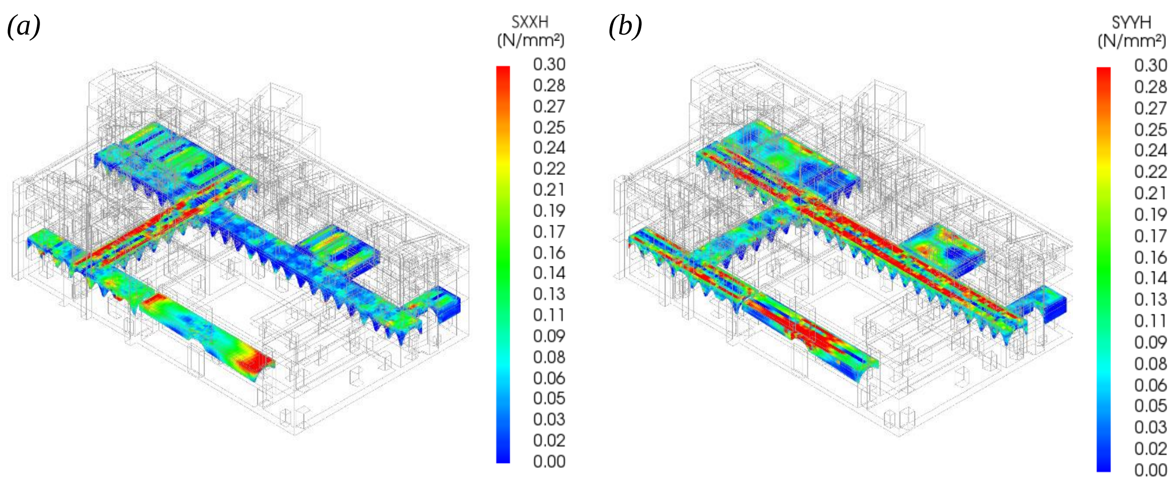

Figure 9. Resulting tensile stresses in the vaults. a) Tensile stress in global X direction (SXXH) resulting from LC1; b) Tensile stress in global Y direction (SYYH) resulting from LC2. The minimum and maximum values on the colour scale are bounded for stress comparison in the two orthogonal directions.

Proceedings of the 2nd Croatian Conference on Earthquake Engineering - 2CroCEE
Zagreb, Croatia - March 22 to 24, 2023
Copyright © 2023 CroCEE
DOI: https://doi.org/10.5592/CO/2CroCEE.2023.23

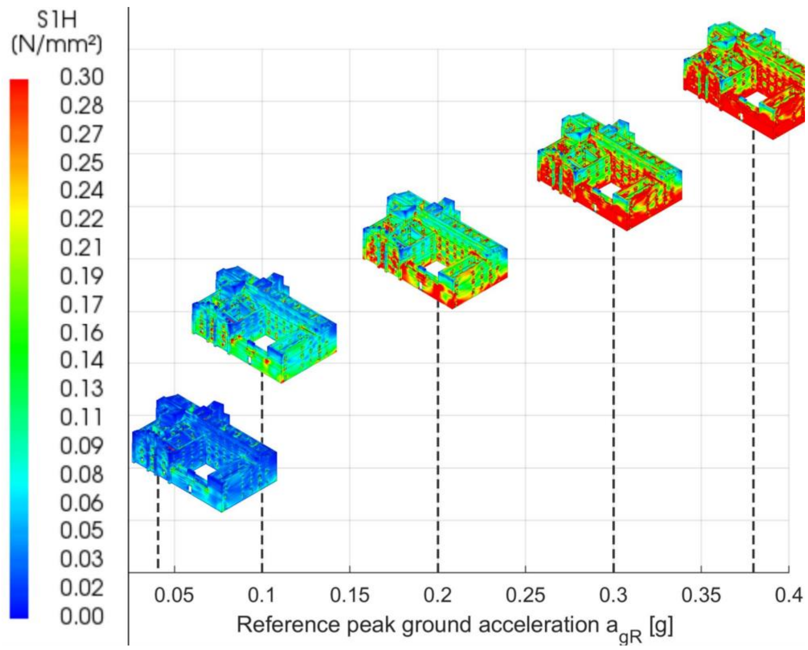

Figure 10. Progression of principal tensile stresses S1H obtained using LC1 by considering different peak ground acceleration values corresponding to the seismic zones in Croatia.

4.2 Out-of-Plane Assessment

The out-of-plane (OoP) assessment of masonry structures is highly dependent on the choice of deformation mechanism whose boundary conditions are usually unknown. In this study, the OoP failure mechanism is assumed based solely on the FEM model results i.e., no observation of cracking is recorded at the site. The assumed mechanism to be activated is dependent on the tensile stress distributions within the localized vulnerable areas. As a result, two mechanisms for two different walls are studied. The acceleration activating the mechanism is estimated based on a linear kinematic analysis using NTC 2018 [22]. The analysis with linear kinematic approach (or linear kinematics) requires the calculation of only the activation multiplier of the mechanism (α_0) and can be used to perform both the verification at the Damage Limit State (activation of the local mechanism) and the Ultimate Limit State. Moreover, the OoP failure is investigated for different levels of a_{gR} by calculating the compliance factor α_{eff} such that, the spectral acceleration required for the activation of local mechanism is smaller than the demand spectral acceleration.

Fig. 11 shows the two probable local failure mechanisms i.e., LM1 and LM2 for the clock and gable walls. The local mechanism (LM1) is the overturning of the whole wall assuming no connection to the orthogonal walls. The local mechanism (LM2) indicates the overturning of the upper part of the clock wall. Fig. 12 illustrates the change in compliance factor for different levels of seismic demand. For the clock wall, the relatively smaller value of α_{eff} in case of LM1 shows that only 0.053g is needed to activate the mechanism, making the clock wall very vulnerable to OoP damages. In the gable wall, LM1 is activated at an a_{gR} of 0.144g. The Croatian NA to Eurocode 8 requires the verification of significant damage (SD) and damage limitation (DL) limit states with peak ground accelerations 0.301g and 0.156g respectively [18]. The small values of compliance factor for both limit states indicate the high vulnerability of the clock and gable wall.

Proceedings of the 2nd Croatian Conference on Earthquake Engineering - 2CroCEE
Zagreb, Croatia - March 22 to 24, 2023

DOI: https://doi.org/10.5592/CO/2CroCEE.2023.23

(a)

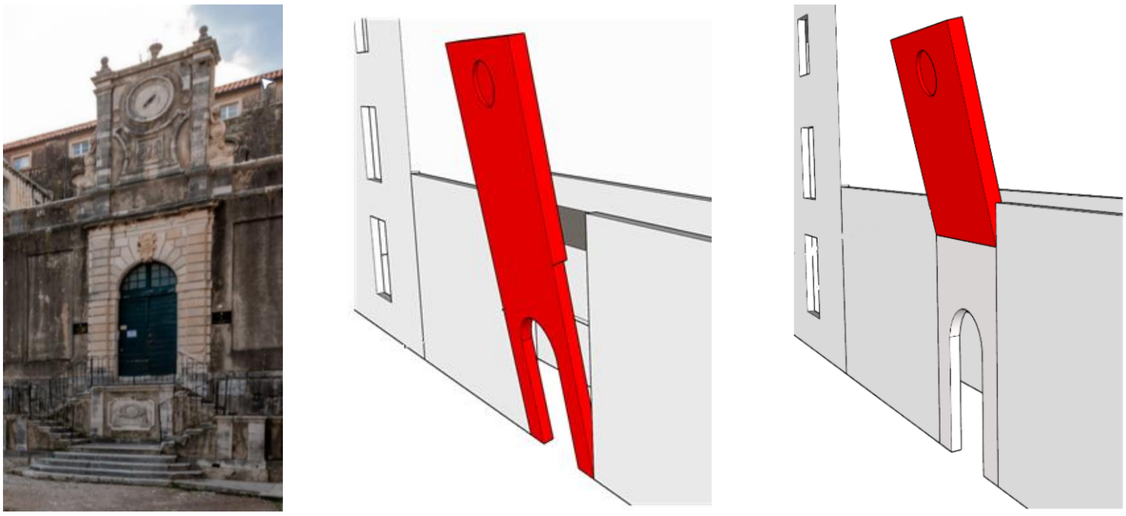

(b)

Figure 11. Description of the assumed local mechanisms LM1 and LM2. a) Clock wall; b) Gable Wall.

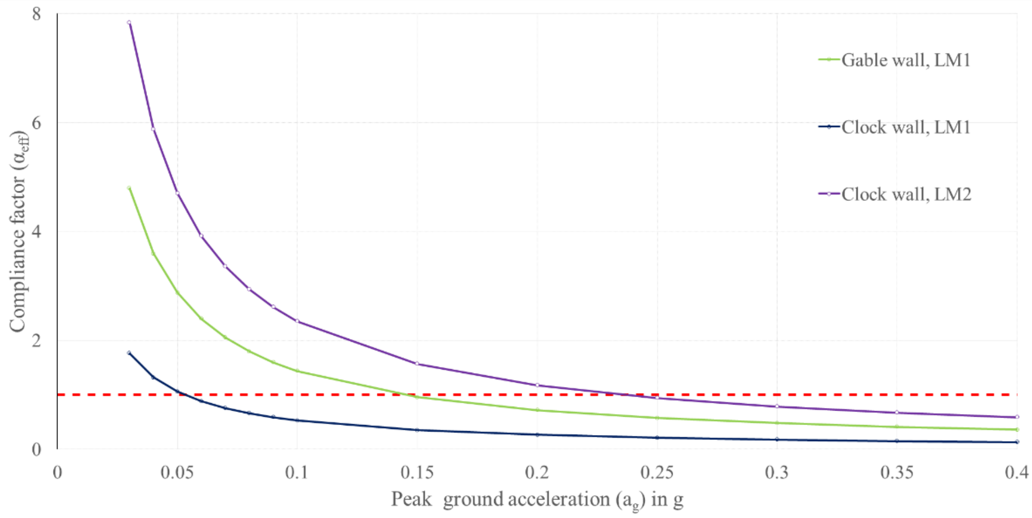

Figure 12. Compliance factor calculated for different demand acceleration levels for clock and gable walls.

Proceedings of the 2nd Croatian Conference on Earthquake Engineering - 2CroCEE
Zagreb, Croatia - March 22 to 24, 2023

DOI: https://doi.org/10.5592/CO/2CroCEE.2023.23

Conclusions

This study presents the earthquake performance assessment of the Jesuit College in Dubrovnik, Croatia using Ambient Vibration Measurements and Finite Element Modelling. The Ambient Vibration Measurements identifies structural frequencies that are excited by low amplitude vibrations required to validate the finite element model. A total of 250 Eigen frequencies are required to accumulate 90% mass participation due to the complexity and size of the numerical model. The free vibration eigenvalue analysis shows the existence of both global and local mode shapes. The mode shapes that excites the major percentage of mass participation in X and Y directions are selected as global modes for the model calibration. Mode shape 1 represents a local bending vibration of the clock wall. Mode shape 2 shows translation in the Y direction. There is no pure translational mode in the X direction; instead, translation in the X direction is accompanied by torsional effects due to the irregularity and the floor plan of the building. In general, several modes describe OoP local vibration of walls.

Several sections of the walls experience stresses that are higher than the material elastic limit. This indicates the presence of cracking that might occur either at the wall surface or internally. From the analysis it is possible to identify zones with high compressive stresses and critical zones of tensile stresses due to the OoP bending of the walls. Compressive stresses are far from the material's elastic limit. The OoP occurs at the west and south wing walls due to the absence of intermediate walls and rigid diaphragms, as well as torsional effects caused by eccentricity. Shear stresses are concentrated in wall sections between adjacent openings i.e., short piers that carry high shear loads in unreinforced masonry structures. The regions with higher shear stresses shows a diagonal trajectory at the piers, and high shear stresses at the bottom of the clock wall due to out-of-plane deformations.

The vaults mainly function as rigid diaphragms, distributing lateral loads and torsional effects to the adjacent walls as shear forces. Therefore, the vaults develop principal tensile stresses as well, which are higher than the material tensile stress limit in some parts of the structure. High tensile stresses are developed in the hallway cross vaults oriented perpendicularly to the main direction of the seismic action between the vault and the lateral walls. The highest stresses are caused by the rigid diaphragm action that the vaults provide as they join portions of long walls that lack of transverse resistance to prevent out-of-plane movement.

Critical zones are identified in order to provide recommendations for strengthening and retrofitting. These are mainly located at the corners of the north wing where the walls intersect with east and west wings, the locations at the north facade of south wing where there is intersection with east and west wings, the walls of the hallway in south wing, the south wing facade, the facade walls of the west wing, and the base of the clock wall and, at the piers between wall openings.

Retrofitting by FRP can be applied to the piers to provide high strength and ductility to minor deformations. Grouting or epoxy injection solution is a low-cost solution that can restore the initial strength state of the wall requiring minimal intervention. The strengthening of wooden diaphragms would enhance the overall seismic response of the building by redistributing the lateral seismic forces along the walls, while dissipate energy through the diaphragm at the same time, reducing the occurrence of out-of-plane bending of the walls. Bracing and tying can provide high resistance against lateral loads, especially in the case of cantilevered walls such as the clock and gable walls. The iron tie-rods installed in the building contributes to the building's resistance to lateral forces by counteracting the out-of-plane bending of the walls. Future retrofitting works involving the tie rods should include experimental determination of the actual tensile forces in the tie-rods.

Acknowledgements

This work has been supported by the Croatian Science Foundation under the research project HRZZ IP-2020-02-3531 "Seismic Risk Assessment of Cultural Heritage Buildings in Croatia-SeisRICHerCRO".

Proceedings of the 2nd Croatian Conference on Earthquake Engineering - 2CroCEE
Zagreb, Croatia - March 22 to 24, 2023

DOI: https://doi.org/10.5592/CO/2CroCEE.2023.23

References

[1] Lourenço PB. Conservation of cultural heritage buildings: Methodology and application to case studies. 1 2013;3(2):98–110. https://doi.org/10.21041/ra.v3i2.46.
[2] Lourenco P, Karanikoloudis G. Seismic behavior and assessment of masonry heritage structures. Needs in engineering judgement and education. RILEM Tech Lett 2018;3:114–20. https://doi.org/10.21809/rilemtechlett.2018.76.
[3] D'Ayala D, Lagomarsino S. Performance-based assessment of cultural heritage assets: outcomes of the European FP7 PERPETUATE project. Bull Earthquake Eng 2015;13(1):5–12. https://doi.org/10.1007/s10518-014-9710-1.
[4] Alban K, Nicola C, Gabriele C, Filippo U. Dynamic testing and monitoring of historic towers for seismic damage detection. In: ; 2017, p. 2564–2577.
[5] Lorenzoni F, Casarin F, Caldon M, Islami K, Modena C. Uncertainty quantification in structural health monitoring: Applications on cultural heritage buildings. Mechanical Systems and Signal Processing 2016;66-67:268–81. https://doi.org/10.1016/j.ymssp.2015.04.032.
[6] Ramos LF, Marques L, Lourenço PB, Roeck G de, Campos-Costa A, Roque J. Monitoring historical masonry structures with operational modal analysis: Two case studies. Mechanical Systems and Signal Processing 2010;24(5):1291–305. https://doi.org/10.1016/j.ymssp.2010.01.011.
[7] Galić J, Vukić H, Andrić D. Structural Assessment of Dubrovnik Cathedral, Croatia. Structural Studies, Repairs and Maintenance of Heritage Architecture XVI 2019;191:467.
[8] Radnić J, Matešan D, Abaza A. Restoration and Strengthening of Historical Buildings: The Example of Minceta Fortress in Dubrovnik. Advances in Civil Engineering 2020;2020:1–17. https://doi.org/10.1155/2020/8854397.
[9] Torres W, Almazán JL, Sandoval C, Boroschek R. Operational modal analysis and FE model updating of the Metropolitan Cathedral of Santiago, Chile. Engineering Structures 2017;143:169–88. https://doi.org/10.1016/j.engstruct.2017.04.008.
[10] Ramos LF, Alaboz M, Aguilar R, Lourenço PB. Dynamic Identification and FE Updating of S. Torcato Church, Portugal. In: Dynamics of Civil Structures, Volume 4. Springer, New York, NY; 2011, p. 71–80.
[11] Standoli G, Salachoris GP, Masciotta MG, Clementi F. Modal-based FE model updating via genetic algorithms: Exploiting artificial intelligence to build realistic numerical models of historical structures. Construction and Building Materials 2021;303:124393. https://doi.org/10.1016/j.conbuildmat.2021.124393.
[12] Markušić S, Ivančić I, Sović I. The 1667 Dubrovnik earthquake–some new insights. Stud Geophys Geod 2017;61(3):587–600. https://doi.org/10.1007/s11200-016-1065-4.
[13] Jemo I, Brigović N. The Restoration of Dubrovnik. The Catalogue of Works in the Historic Centre of Dubrovnik from 1979 till 2009.
[14] SeisRICHerCRO. Seismic Risk Assessment of Cultural Heritage Buildings In Croatia. [January 14, 2023]; Available from: https://seisrichercro.wordpress.com/.
[15] Penava D, Vrban A, Uglešić J, Stanko D, Markušić S. Episcopal seminary building and classical gymnasium (Jesuit college) in Dubrovnik construction 1662-1765 in terms of contemporary earthquake resistant design supported by measurements // Proceedings of the 10th International Congress of Croatian Society of Mechanics / Skozrit, Ivica ; Tonković, Zdenko ; Sorić, Jurica (ur.). Pula: Croatian Society of Mechanics, 2022. str. 39-40.
[16] Horvat LK, Haničar BI, Vareško G. The building of the Episcopal Seminary and Classical Gymnasium Jesuit College in Dubrovnik. Conservation study with guidelines for restoration (in Croatian: Zgrada biskupskog sjemeništa i klasične gimnazije (Isusovački kolegij) u Dubrovniku. Konzervatorska studija sa smjernicama za obnovu). Zagreb, Croatia; 2022.
[17] Morić D. Floor Structures and Seismic Resistance of Cultural Heritage Stone Masonry Buildings; 2003.
[18] Eurokod 8: Projektiranje potresne otpornosti konstrukcija -- 1. dio: Opća pravila, potresna djelovanja i pravila za zgrade (EN 1998-1:2004+AC:2009).
[19] Eurokod 8: Projektiranje potresne otpornosti konstrukcija -- 3. dio: Ocjenjivanje i obnova zgrada (EN 1998-3:2005+AC:2010).
[20] Ivančić I, Herak D, Herak M, Allegretti I, Fiket T, Kuk K et al. Seismicity of Croatia in the period 2006-2015. geofizika 2018;35(1):69–98. https://doi.org/10.15233/gfz.2018.35.2.
[21] Markušić S, Stanko D, Korbar T, Sović I. Estimation of near-surface attenuation in the tectonically complex contact area of the northwestern External Dinarides and the Adriatic foreland. Nat. Hazards Earth Syst. Sci. 2019;19(12):2701–14. https://doi.org/10.5194/nhess-19-2701-2019.
[22] NTC 2018 – Nuove norme sismiche per il calcolo strutturale.